Carbohydrate Polymers 94 (2013) 261–271

Contents lists available at SciVerse ScienceDirect

Carbohydrate Polymers

journal homepage: www.elsevier.com/locate/carbpol

# Homogeneous synthesis of chitin-based acrylate superabsorbents in NaOH/urea solution

Tingguo Liu[a,*], Liwu Qian[a], Bin Li[b,1], Jing Li[b], Kunkun Zhu[b], Hongbing Deng[b], Xiaohong Yang[a], Xin Wang[a,**]

[a] Provincial-Level Experimental and Teaching Demonstration Center of Chemical Materials & Engineering, Chizhou University, Anhui Chizhou 247100, People's Republic of China
[b] College of Food Science and Technology, Huazhong Agricultural University, Wuhan 430070, People's Republic of China

ARTICLE INFO

*Article history:*
Received 10 October 2012
Received in revised form 2 January 2013
Accepted 8 January 2013
Available online 23 January 2013

*Keywords:*
Chitin
Alkali-freezing
Superabsorbent polymers
Graft polymerization
Hydrogels

ABSTRACT

A modified freezing–thawing cyclic (FTC) process was applied to dissolve the chitin in NaOH/urea solution. A transparent homogeneous solution was obtained. It was utilized directly for preparing the superabsorbent polymers (SAPs) by grafting copolymerization under static solution conditions without nitrogen protection. The acrylic acid was used conveniently without prior neutralization. The final products existed as hydrogels without excess reagent emissions. The adsorption capacity and yield of SAP that was prepared in the optimum conditions was 2833 g/g and 81.65%, respectively, higher than one-time FTC program prepared with 2527 g/g and 15.44%. Furthermore, it formed a uniform and transparent gel without any residual chitin particles. The regenerated chitin and SAPs were characterized by SEM, FTIR, XRD, and TG. The samples prepared by the new method presented a more amorphous state with good thermal stability, suggesting that this convenient preparation method for a potential industrial application's pathway.



## 1. Introduction

Superabsorbent polymers (SAPs) are novel functional polymer materials with a unique three-dimensional network structure and an appropriate degree of crosslinking (Chen, Liu, Tan, & Jiang, 2009). They can absorb and retain several hundred times of a liquid relative to their own dry weight, and it is hardly to remove the absorbed water even under some pressure or heating (Liu, Wang, & Wang, 2007; Yang, Ma, & Guo, 2011). Superabsorbent polymers have many excellent properties than traditional water absorption materials (such as sponge, cotton, pulp, wood, soil, and silica gel). They are widely used in many fields, especially in the fields of personal care, agriculture, forestry and horticulture, which has become an indispensable material (Liu et al., 2007; Zhang, Wang, & Wang, 2007). The market share and yields of synthetic polymers are rather high owing to their powerful absorbing capacities, low-cost and high gel strength. However, most raw materials of the synthetic SAPs are from the petroleum processing byproducts such as acrylic acid, acrylamide, and acrylonitrile, which are not biodegradable in nature (Liu et al., 2007; Zhang et al., 2007). With the gradual depletion of fossil energy, a higher demand on resources and social sustainable development has been put forward in recent years. The development and application of biomass energy resources as novel materials are one of the new research hotspots. It is expected to replace the widespread application of synthetic polymers with the gradual in-depth study of the natural polymers. It is urgent that the green SAPs has been synthesized with some non-toxic, biodegradable, low-cost natural polymeric materials. The frequently exploited natural polymers have been studied for a long time, including starch (Nakason, Wohmang, Kaesaman, & Kiatkamjornwong, 2010; Zou et al., 2012), cellulose (Chang, Duan, Cai, & Zhang, 2010; Ma et al., 2011), protein (Zhang, Cui, Yin, & Zhou, 2011a; Zhang et al., 2011b), chitosan (Chen et al., 2009; Chen & Tan, 2006; Liu et al., 2007; Zhang et al., 2007), collagen (Sadeghi & Ghasemi, 2012; Sadeghi & Hosseinzadeh, 2010) and some other biological resources.

Chitin is the second most abundant biopolymer (after cellulose) and is the only natural basic polysaccharide widely found in nature (Muzzarelli et al., 2012). It is usually extracted from shrimp and crab shells of waste materials from the seafood processing industry (Lin, Lin, & Chen, 2009). Due to its special structure, there are plenty of unique properties. As safe biomaterials, it has been widely applied in the light industry, biomedicine, pharmaceutical,

* Corresponding author.
** Corresponding author. Tel.: +86 15905660718.
*E-mail addresses:* liutg137@hotmail.com (T. G. Liu), libinfood@mail.hzau.edu.cn (B. Li), wangxin164@sina.com (X. Wang).
[1] Tel.: +86 13296597469; fax: +86 027 87282966.

0144-8617/$ – see front matter © 2013 Elsevier Ltd. All rights reserved.
http://dx.doi.org/10.1016/j.carbpol.2013.01.010

cosmetic, environmental protection, agricultural, and many other fields (Cho, Jang, Park, & Ko, 2000; Liu et al., 2009; Muzzarelli, 2011, 2012). However, it is perhaps the least exploited biomass source to date (Chang, Chen, & Zhang, 2011; Pillai, Paul, & Sharma, 2009). A large number of abandoned shrimp and crab shells are not only an enormous waste of resources, but also a heavy burden to the environment. Therefore, it is still a challenging research to accelerate the development of chitin- or chitosan-based new products and to increase the applications of them in broader fields. The chemical structure of chitosan is similar to cellulose to some degree. Like cellulose, it can also be prepared as superabsorbent polymers through radical graft polymerization with vinyl monomers and crosslinking (Wang, Chen, Zhang, & Yu, 2008). Furthermore, due to the existence of amine groups, chitosan based SAPs not only possesses a good water absorbent, but also has antibacterial activities (Elkholy, Khalil, Elsabee, & Eweis, 2007), which make it very suitable to be used in infant diapers, feminine hygiene products and other special fields (Zhang et al., 2007).

As the precursors of chitosan, chitin can also be prepared SAPs, and it should be more competitive than chitosan. However, chitin is insoluble in common solvents because of its strong intra- and inter-molecular hydrogen bonds (Austin, Brine, Castle, & Zikakis, 1981). Therefore, the usage of chitin as a raw material for graft copolymerization was restricted, and the literature on the preparation of SAPs was even more scarce. Nevertheless, there are still many researchers prepared chitin grafted copolymers between chitin and vinyl monomers under heterogeneous (Yazdani-pedram, Lagos, Campos, & Retuert, 1992) or homogeneous phase (Kim, Ha, & Jo, 2002). The grafted polymers revealed better affinity for solvents, hygroscopicity (Kurita, Kawata, Koyama, & Nishimura, 1991), paraquat (Hsu et al., 2013), metal binding ability (Furlan, Fávere, & Laranjeira, 1996) and efficiently dissociated and dispersed homogeneously in basic water (Ifuku, Iwasaki, Morimoto, & Saimoto, 2012). The results indicated that the graft copolymer was promising as a paraquat adsorbent, a glass cements, a wound dressing (Tanodekaew et al., 2004) or a novel superabsorbent hydrogels (Yoshimura, Uchikoshi, Yoshiura, & Fujioka, 2005).

The previous studies suggested that it was feasible to prepare superabsorbent polymers by grafting with chitin and hydrophilic monomers. Nevertheless, most of the earlier studies were carried out under heterogeneous conditions, and the maximum water absorbency was only about 300 times of its own dry weight. It has been reported that alkali-freezing treatment can reduce or break crystalline linkages between the sheets of chains in chitin, and the existence of alkali can enhance the extent of decrystallization. Then, a transparent alkaline solution was obtained (Hu et al., 2007; Ding et al., 2012).

In this work, a novel superabsorbent was designed through grafting acrylic acid (AA) onto chitin (CH) with suitable crosslinking in NaOH/urea solution without nitrogen protection. Chitin was dissolved in an 8 wt% NaOH/4 wt% urea aqueous solution by using a modified two times freezing–thawing cyclic (FTC) treatment. The structural changes before and after grafting polymerization were estimated, and the effects of FTC treatments on the condensed structure of chitin were also investigated. It is expected to provide a simple methodological and technical reference for the preparation of superabsorbent, the in-depth development and applications of chitin.

## 2. Materials and methods

### 2.1. Materials

Chitin powder derived from shrimp shells was purchased from Zhejiang Yuhuan Biochemical Co. (PRC). The raw material is evaporated under a vacuum at 60 °C for 48 h and grounded with a laboratory scale hammer mill without further purification. The final product was powder screened to about 80 meshs, with a degree of deacetylation (DDA) of 21.11 ± 0.59%, as determined by alkalimetric estimation (Liu et al., 2009). The viscosity-average molecular weight was $1.20 \times 10^6$, measured in an Ubbelohde viscometer. Acrylic acid monomer (AA, AR), ammonium persulfate (APS, AR) and N,N′-methylenebisacrylamide (MBA, CP) was supplied by Shanghai Reagent Corp. (Shanghai, China) without additional treatment. All other commercially available solvents and reagents were analytical grade, and were used directly without further purification. Running water is potable water in ChiZhou city (China), and the electrical conductivity is 282 μS/cm. The normal saline was prepared by dissolving 0.90 g sodium chloride (NaCl) in 99.10 ml distilled water. And the artificial urine was prepared by dissolving 1.94 g urea, 0.11 g magnesium sulfate heptahydrate ($MgSO_4 \cdot 7H_2O$), 0.08 g NaCl, 0.06 g calcium chloride ($CaCl_2$) in 97.81 ml distilled water. Unless otherwise specified, double distilled water (the electrical conductivity is 6.40 μS/cm) was used throughout the experimental process.

### 2.2. Preparation of chitin solution

Chitin solution and regenerated chitin were prepared according to Scheme 1. Chitin powder was dispersed in 40 wt% NaOH aqueous solution with the feed liquid ratio being 1:4 and soaked at room temperature for 8 h in order to make NaOH fully penetrate into chitin particles. After about 1 day freezing at −18 °C, the sample was immediately thawed at 40 °C until the center temperature went up to 40 °C (Liu et al., 2009). This was the first-time freezing–thawing-cyclic (FTC) treatment. Then repeating the above FTC treatment once again, diluted it with urea aqueous solution. Subsequently, a clear and transparent chitin homogeneous solution was obtained, with 3 wt% chitin, 8 wt% NaOH and 4 wt% urea. A minor portion of chitin solution was removed for its structural analysis. It was precipitated and washed by 70% EtOH until a decanted solution reached pH 7. Subsequently, it dehydrated by 95% and anhydrous ethanol and then dried at 60 °C for 48 h under diminished pressure. Finally, the regenerated chitin was ground and marked as CH1. In order to compare with the method reported throughout the literature (Hu et al., 2007), another sample was also prepared. Chitin powder was directly dispersed in 8 wt% NaOH/4 wt% urea solution, then freezing at −18 °C overnight (Hu et al., 2007). After thawing, a heterogeneous solution was obtained, and the regenerated chitin was marked as CH2.

### 2.3. Preparation of superabsorbent polymers

Superabsorbent polymers were prepared according to Scheme 1. The procedure for synthesizing SAP1 was described in detail as an example. The graft copolymerization was performed in a 100 ml beaker, which was placed in a temperature-controlled water bath, without nitrogen protection. Firstly, 50 mg APS ($m_{CH}$:$m_{APS}$ = 12:1) was added into 20 g chitin solution (including 0.60 g CH1, 1.60 g NaOH and 0.80 g urea) and stirred for 0.5 h at room temperature. Then 10 mg MBA ($m_{CH}$:$m_{MBA}$ = 60:1) and 8.4 ml AA ($m_{CH}$:$m_{AA}$ = 1:14, mixed with 37.8 ml $H_2O$) was added into the mixed solution with string, finally sealed with plastic film and maintained at 65 °C for 5 h. After graft copolymerization, the reaction mixture was cooled to room temperature and a hydrogel was obtained. It subsequently poured out the excessive solution which cannot form a hydrogel. The residual hydrogel was soaked in 75% ethanol for 12 h, then cut into small pieces and soaked in 75% ethanol for 5 h (two times) to remove nongrafted polyacrylic acid and other chemicals. The precipitates were collected and suspended in anhydrous ethanol for 2 h (two times) to remove

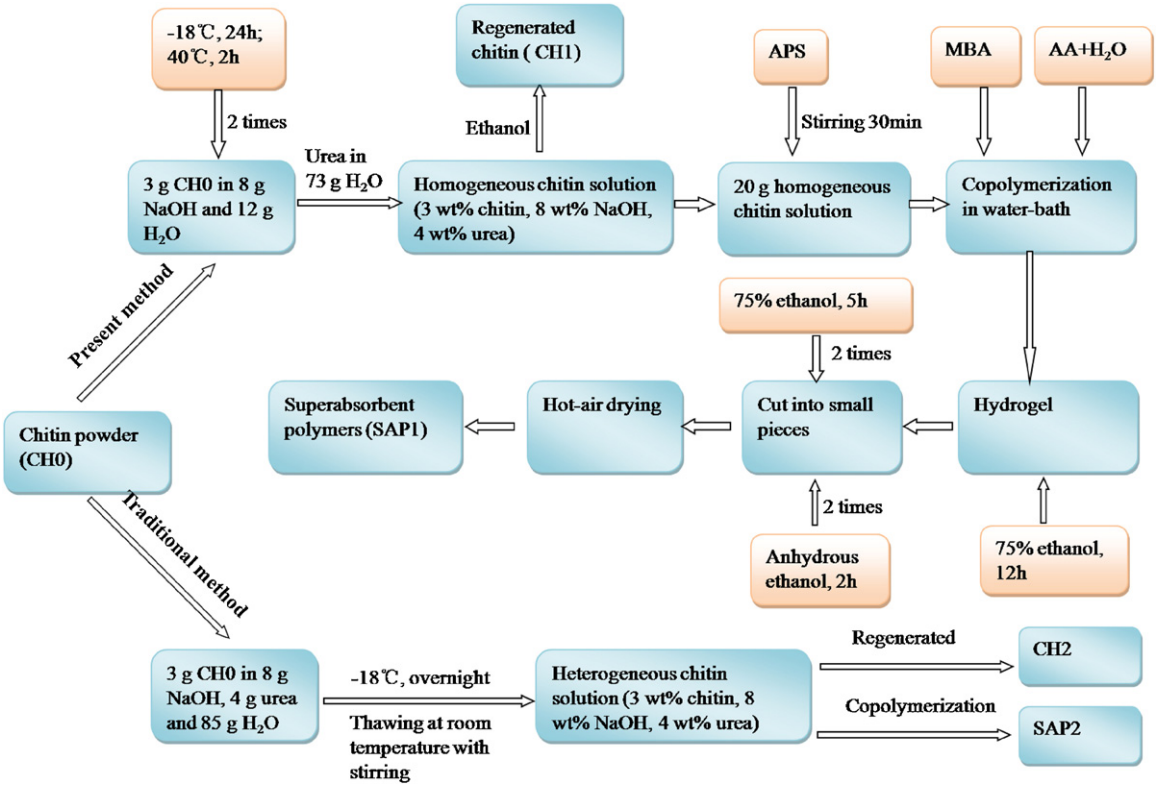


**Scheme 1.** Preparation of regenerated chitin and chitin-based superabsorbent polymers.

water, and then dried overnight at 60 °C in a digital display electric thermostat blast oven. The yield was calculated as follows:

$$\text{Yield}\ (\%) = \frac{\text{Total weight of the final SAPs products}}{\text{Total weight of the raw materials}} \times 100$$

$$= \frac{m_{\text{SAPs}}}{m_{\text{CH}} + m_{\text{APS}} + m_{\text{MBA}} + m_{\text{AA}} + m_{\text{NaOH}} + m_{\text{urea}}} \times 100$$

SAP2 was carried out as follows: 0.60 g CH0 was mixed with NaOH/urea aqueous solution (including 1.6 g NaOH, 0.8 g urea and 17.0 ml $H_2O$) and froze at −18 °C for overnight. Equivalent amounts of APS, MBA and AA were added after thawing according to the procedure of SAP1. The blank controlled sample (PAA) was carried out in a similar way without chitin.

### 2.4. Determination of the water absorption capability

The distilled water absorbency ($Q_d$) of superabsorbent composite was measured as followed (Zhang et al., 2007; Chen et al., 2009). Sample (0.0500 g) was immersed in distilled water (200 ml) at room temperature for 12 h to reach swelling equilibrium. Every sample was carried out in triplicate. The residual water was removed by filtrating with 120-mesh nylon screen. The weight of the swollen polymer was measured until water ceased to drop (about 4 h), and the water absorbency was calculated according to the following equation:

$$Q_d = \frac{m_2 - m_1 - m_0}{m_0}$$

where $Q_d$ is the water absorbency of the sample in distilled water. $m_0$ (g) is the weight of the dry SAPs, $m_1$ (g) is the weight of the nylon screen, and $m_2$ (g) is the total weight of the swollen SAPs and nylon screen, respectively.

According to the same determine procedure for $Q_d$, 0.2000 g sample and 200 ml liquid was used for determining the water absorbency in running water, normal saline and artificial urine, respectively.

### 2.5. Macroscopic and SEM analysis

A small piece sample (about 0.03 g) was immersed in the distilled water, which was taken out and photoed by a digital camera (IXUS 300HS, Canon, Japan) after 5 min, and immersed in water again. After about 24 h, the sample absorbed water and formed a good hydrogel, and was taken photographs again.

The microstructure of a dry SAP sample was investigated by means of a JSM-6700F field emission scanning electron microscope (JEOL Ltd., Japan). Before SEM observation, the dehydrated sample was grounded into powder, fixed on aluminum stubs and coated with gold. Subsequently, its microstructure was observed and photographed (Chen et al., 2009; Zhang et al., 2007).

### 2.6. Characterization

Powder X-ray diffraction (XRD) profiles were measured with a JDX-10P3A diffractometer (JEOL Ltd., Japan) under 20 °C. The operating conditions were 30 mA, 35 kV, DS/SS = 1°, RS = 0.3 mm with Cu $K\alpha_1$ radiation at $\lambda$ = 1.54184 Å. The scanning rate was 4°/min and the diffraction angle ($2\theta$) ranged from 4 to 60° with resolution of 0.02° (Hu et al., 2007). All data were procured using the MDI jade software package (jade 5.0, Materials Data Inc., Japan).

The FT-IR spectra was recorded with KBr pellets on a FT-IR spectrometer (IR 200, Nicolet, USA) at an ambient temperature, at 32 accumulate scans in the region from 4000 to 400 $cm^{-1}$, with a resolution of 4 $cm^{-1}$ were averaged and referenced against air (Liu et al., 2009).

The measurement of thermal stability of samples (around 10 mg) was carried out using a HTG-1 thermogravimetric analyzer (Beijing Scientific Instrument Factory, China), with a temperature

**Table 1**
Orthogonal experiment results.

| | | A | B | C | D | E | F | Water absorbency in d-water (g/g)[a] | Yield (%) |
|---|---|---|---|---|---|---|---|---|---|
| | | $m_{CH}$:$V_{AA}$(g/ml) | $m_{CH}$:$m_{APS}$(mg/mg) | $m_{CH}$:$m_{MBA}$(mg/mg) | Temperature (°C) | Time (h) | $m_{CH}$:$m_{NaOH}$(g/g) | | |
| 1 | | 1 (1:10) | 1 (20:1) | 1 (75:1) | 1 (55) | 1 (4) | 1 (3:6) | – | 0.00 |
| 2 | | 1 | 2 (15:1) | 2 (60:1) | 2 (60) | 2 (5) | 2 (3:8) | 2282 ± 61 | 49.93 |
| 3 | | 1 | 3 (12:1) | 3 (50:1) | 3 (65) | 3 (6) | 3 (3:10) | 1318 ± 20 | 92.44 |
| 4 | | 2 (1:12) | 1 | 1 | 2 | 2 | 3 | 1813 ± 71 | 43.60 |
| 5 | | 2 | 2 | 2 | 3 | 3 | 1 | 1803 ± 52 | 79.89 |
| 6 | | 2 | 3 | 3 | 1 | 1 | 2 | 1472 ± 48 | 31.28 |
| 7 | | 3 (1:14) | 1 | 2 | 1 | 3 | 2 | 2877 ± 61 | 9.35 |
| 8 | | 3 | 2 | 3 | 2 | 1 | 3 | 2407 ± 37 | 59.52 |
| 9 | | 3 | 3 | 1 | 3 | 2 | 1 | 2482 ± 49 | 86.25 |
| 10 | | 1 | 1 | 3 | 3 | 2 | 2 | 1906 ± 69 | 73.27 |
| 11 | | 1 | 2 | 1 | 1 | 3 | 3 | 2093 ± 39 | 23.40 |
| 12 | | 1 | 3 | 2 | 2 | 1 | 1 | 2373 ± 35 | 56.33 |
| 13 | | 2 | 1 | 2 | 3 | 1 | 3 | 1983 ± 18 | 82.60 |
| 14 | | 2 | 2 | 3 | 1 | 2 | 1 | 2053 ± 37 | 32.34 |
| 15 | | 2 | 3 | 1 | 2 | 3 | 2 | 2277 ± 63 | 73.95 |
| 16 | | 3 | 1 | 3 | 2 | 3 | 1 | 1678 ± 48 | 61.51 |
| 17 | | 3 | 2 | 1 | 3 | 1 | 2 | 2176 ± 42 | 82.50 |
| 18 | | 3 | 3 | 2 | 1 | 2 | 3 | 2061 ± 22 | 51.14 |
| $Q_d$[a] | $k_1$ | 1662 | 1710 | 1807 | 1759 | 1735 | 1732 | | |
| | $k_2$ | 1900 | 2136 | 2230 | 2138 | 2100 | 2165 | | |
| | $k_3$ | 2280 | 1997 | 1806 | 1945 | 2008 | 1946 | | |
| | $R$ | 618 | 426 | 424 | 379 | 365 | 433 | | |
| $Y$[b] | $k'_1$ | 49.23 | 45.06 | 51.62 | 24.59 | 52.04 | 52.72 | | |
| | $k'_2$ | 57.28 | 54.60 | 54.87 | 57.47 | 56.09 | 53.38 | | |
| | $k'_3$ | 58.38 | 65.23 | 58.39 | 82.83 | 56.76 | 58.78 | | |
| | $R'$ | 9.15 | 20.17 | 6.77 | 58.24 | 4.72 | 6.06 | | |
| $Q$ | | $A_3$ | $B_3$ | $C_2$ | $D_3$ | $E_2$ | $F_2$ | | |

[a] $Q_d$, water absorbency in d-water, mean ± standard deviation, $n = 3$; $k$, the average of the same level; $R$, the difference of maximum and minimum values; $Q$, the optimum conditions.
[b] Y, yield.

range of 30–650 °C at a heating rate of 10 °C/min under a dry air atmosphere (Zhang et al., 2007).

## 3. Results and discussion

### 3.1. Preparation of superabsorbent polymers

Generally, it is a typical free radical polymerization that graft the water-soluble vinyl monomer onto the backbone of cellulose-like polysaccharide by the redox initiator. Most of the graft co-polymerization reacts by chain mechanism. It can be summarized as chain initiation, chain propagation, chain transfer, and crosslinking. APS is a typical thermally dissociated initiator, which can generate $SO_4^{-\bullet}$ primary free radicals by decomposition under suitable temperature. First, the primary radicals are attracted by the $-NH_2$ or $-NHCOCH_3$ groups in the chitin ring. Second, they attack the C-1 or C-4 atoms and transfer the radicals to the carbon atoms by subtracting the hydrogen from it. Finally, the presence of free radical at C-1 or C-4 cause breakage of the adjacent C—O—C glycosidic bonds in the main chain, creating new macro radicals at the chain ends (Hsu, Don, & Chiu, 2002). Subsequently, it will react with acrylic acid molecules, followed by propagation leading to the growth of a branched chain, and then moderately crosslinked with a crosslinker. A superior three-dimensional network structure was formed, and the superabsorbent polymer was obtained (Chen et al., 2009; Yang et al., 2011). In addition, PAA-based superabsorbent composite is a typical ionic polymer. According to Flory's network theory, the fixed charges on the polymeric network play an important role in the swelling of the SAPs. The charges can be adjusted by changing the molar ratio of NaOH to AA while it partially neutralized (Chen et al., 2009). Therefore, the factors that affect the final water absorbency of SAPs were investigated, including the amount of AA monomer (marked as "A"), initiator ("B"), crosslinker ("C"), reaction temperature ("D"), reaction time ("E") and the amount of NaOH ("F"). Thus, based on our previous work with superabsorbent composite and chitin, a $L_{18}(3^6)$ orthogonal experiment design was applied to investigate the effects of different reaction conditions on the water absorbency and yield, the result of which was exhibited in Table 1. Under the experimental conditions, the ratio of $m_{CH}$ to $V_{AA}$ was the most significant factor on the water absorbency. The dosage of NaOH followed, and the effect of reaction time were the relative trivial factor. For yield, the most significant factors were reaction temperature and the usage of the initiator. On the contrary, they were not the especially significant factors on the water absorbency. The effect factors on the water absorbency can be arranged in order as $A \gg F \sim B \sim C > D \sim E$. Like wise the yield, the order was $D \gg B \gg A > C \sim F > E$.

#### 3.1.1. Effects of the amount of AA on the water absorbency and yield of SAPs

The water absorbency and product yield increased continuously with the increase of the amount of AA in Table 1. Apparently, more and more hydrophilic groups such as $-COO^-$ and —COOH were grafted onto the chitin skeleton. This due to the increased monomer concentration promoted by the monomer molecules' accumulation close to the chitin backbone. There are adequate PAA chains to participate in the formation of a fine network structure, leading to an increase of the water absorbency and yield. However, the water absorbency and the yield augmented insignificantly with adding the amount of AA continuously. It may be ascribed to preferential homopolymerization and the enhanced chance of the chain transferring to the monomer molecules, rather than graft copolymerization (Ma et al., 2011; Zhang et al., 2007).

*3.1.2. Effects of the amount of NaOH on the water absorbency and yield of SAPs*

Although the activity of hydroxyl on the N-acetyl glucosamine residues in chitin molecules was significantly weaker than that of small-molecule hydroxyl, it could also be substituted and formed an alkali-chitin. Furthermore, it can be dissolved into aqueous NaOH as the alkoxide form, with only a little NaOH being used to form a sodium-chitin between $C_6$—OH and NaOH, and most of the redundant NaOH being applied to neutralize AA. The neutralization degree of AA increased with the augment of the dosage of NaOH. The water absorbency rapidly increased with the increase of the amount of NaOH until the maximum water absorbency was reached (Table 1). In contrast, the effect of the NaOH dosage on the yield increased gently with the NaOH increasing. Indeed, the proportion of two different hydrophilic groups —COOH and —COONa in the SAPs can be adjusted by changing the neutralization degree of AA. The content of —COONa groups increased with the augment of the neutralization degree of AA, resulting in the increase of the electrostatic repulsion and the osmotic pressure difference between the inside and outside the network, which ultimately lead to an increase of equilibrium water absorbency. However, further augment of the neutralization degree of AA, which means more $Na^+$ ions in the polymeric network would react with the —COOH groups led to the augment of water solubility of SAPs. As a result, the electrostatic repulsion and the osmotic pressure of the gel phases reduced, leading to the water absorbency to decrease immediately (Chen and Tan, 2006; Zhang et al., 2007).

*3.1.3. Effects of the amount of APS on the water absorbency and yield of SAPs*

The water absorbency increased as the amount of initiator APS increased (Table 1). When the amount of APS was higher than the maximum point, the water absorbency decreased slowly with further increase of APS. In contrast, the yield increased rapidly with the increase of the amount of initiator APS, and it is the second most important factor that affects the yield of SAPs after the factor of reaction temperature. In fact, the initiator is mainly by impacting the linear relative molecular weight of the SAPs to affect its water absorbency. When the reaction temperature is constant, more initiators are needed and more free radicals are generated by heating decomposition. It in turn creates more macro radicals in the main chain of chitin and shorter average kinetic chain length of PAA is made. More graft polymerization occurred and more stable network structures formed, which was helpful to the augment of the water absorbency and yield (Ma et al., 2011). When the amount of the initiator is little, the yield is lower, even no SAP product has been obtained (the No. 1 experiment in Table 1). Fewer free radicals were generated by heating decomposition, resulting in fewer reactive radical sites and smaller crosslinking density, leading to less hydrogel forming. However, if the amount of initiators increased further, more radicals would enhance the terminating step via bimolecular collision, which resulted in the decrease of the main chain length and the increase of the crosslinking density (Chen and Tan, 2006). Therefore, the water absorbency of the polymer decreased, while the yield increased slowly.

*3.1.4. Effects of the reaction temperature on the water absorbency and yield of SAPs*

The reaction temperature was the most significant factor for the yield, as shown in Table 1. The yield increased with the temperature increasing because of the improvement of polymerization rate. However, the water absorbency increased with the temperature reached to 60 °C, then it decreased with further increasing. In the radical polymerization reaction, the monomer polymerization rate depends largely on the decomposition rate of the initiator. APS is a typical thermo-sensitive initiator, which can release more radicals resulting in a more intense polymerization reaction with the temperature increasing. However, when the reaction temperature was too high, more activation energy resulting in a large excess of free radicals, the polymerization rate, cross-linking points and homopolymer in the hydrogel increased (Chen et al., 2009; Chen and Tan, 2006; Ma et al., 2011). So, the water absorbency of the SAP decreased with the yield of the SAP increasing. When the reaction temperature was lower, the free radicals generated by heating decomposition were fewer, the chain initiation reaction was slower, fewer monomers participated in the graft polymerization reaction within a certain time, resulting in the incompletion of the polymerization reaction and the falling of the yield. Furthermore, the reaction generally needs to be carried out under nitrogen protection, due to the radical polymerization reaction is affected by the influence of oxygen. Nevertheless, in this work, all experiments were carried out in a thermo-constant temperature water bath without any protection, so, when the reaction temperature was low with fewer initiators, the yield was low and even no SAPs were obtained (No. 1 in Table 1).

*3.1.5. Optimization of the reaction parameters*

The experimental program based on orthogonal test results with maximum absorbency was $A_3B_2C_2D_2E_2F_2$, but the yield was less than 60%. Conversely, the desirable program with maximum yield was $A_3B_3C_3D_3E_3F_3$, with the water absorbency just about 1800 times. Therefore, considering the factors impact on the water absorbency and the yield of SAPs, the optimal program was determined as $A_3B_3C_2D_3E_2F_2$. The optimum reaction conditions were performed as follows: the amount of CH0 was 0.6 g, $m_{CH}$:$V_{AA}$ = 1:14, $m_{CH}$:$m_{APS}$ = 12:1, $m_{CH}$:$m_{MBA}$ = 60:1, $m_{CH}$:$m_{NaOH}$ = 3:8; the amount of urea was 0.8 g; the reaction temperature and time were 65 °C and 5 h, respectively. Under these conditions, a chitin-based superabsorbent polymer (SAP1) was prepared without nitrogen protection, and it could absorb about 2800 times water. A control sample (SAP2) was also prepared according to the literature method (Hu et al., 2007) for preparing chitin-alkaline solution. The detailed results are shown in Table 2.

*3.2. Morphological analysis*

In order to understand the shape change of the SAP before and after absorption, the samples before and after swelling in distilled water were photographed with a digital camera. Both the dehydrated sample SAP1 and SAP2 had a small volume with a high crosslinking degree and similar shape, even when it was immerged in distilled water for a little time (less than 5 min, in Fig. 1). However, when it fully absorbed water, the internal network structures of the both SAPs expanded, and water was kept inside the network. A very good transparent hydrogel was formed in SAP1 (Fig. 1a), whereas in SAP2, a lot of visible chitin granules can be seen in the hydrogel (Fig. 1b). Recently, Hu et al. reported that 8 wt% NaOH/4 wt% urea can be used as an excellent solvent for chitin, but it was still difficult to successfully achieve according to the literature (Hu et al., 2007). Perhaps, It has not been reported that some factors influence the solubility of chitin in this novel solvent. Therefore, the SAP2 sample that prepared according to the literature method was actually synthesized under heterogeneous phase conditions. Only a part of PAA chains grafted onto the surface of the chitin granule with a small amount of chitin particles were wrapped by PAA network, and the proposed schematic structure of the SAP2 was shown in Fig. 1d. It is highly different from SAP1 as shown in Fig. 1c.

The micrographs of regenerated chitin (CH1 and CH2), superabsorbent polymers (SAP1 and SAP2), and blank control sample (PAA) are shown in Fig. 2. It has been reported that powdered chitin extracted from shrimp shells has an impacted multilayered

**Table 2**
The optimal and controlled experiment results, respectively.

| Sample | Yield (%) | Water absorbency (g/g) | | | |
|---|---|---|---|---|---|
| | | Distilled water | Running water | 0.9% NaCl | Artificial urine |
| SAP1 | 81.65 | 2833 ± 92 | 544 ± 22 | 79 ± 2 | 88 ± 1 |
| SAP2 | 15.44 | 2527 ± 170 | 456 ± 48 | 85 ± 6 | 77 ± 2 |
| PAA | 43.30 | 2553 ± 151 | 508 ± 32 | 106 ± 9 | 105 ± 10 |

structure. It revealed a distinct change of CH1 with respect to the crude chitin, after FTC treatment a new, loose and undulant surface structure had been formed. It was convenient for the penetration of reagents into the chitin molecular chain and was helpful to accelerate chemical modification reaction rate. After the modification, the surface became smooth, tight and porous, which was one of the reasons that the water absorption rate of SAP1 is not high. This change in surface morphology supported the occurrence of graft polymerization (Chen et al., 2009). However, the surface of CH2 is highly similar to the curd chitin, whereas it is slightly looser than the structure of the raw materials. After polymerization, it can be seen the chitin particles were in the center of a porous PAA network structure, maybe the PAA chains only grafted onto the surface of chitin granules (SAP2). This result can support the speculation on SAP2 structure in Fig. 1d.

### 3.3. Characterization

It has been revealed in plenty of research that the existence and growth of ice crystals cause mechanical damage on the microstructure of carbohydrate polymers during freezing treatment. Furthermore, it has been reported that with alkali-freezing treatment, the crystalline linkages among the sheets of chains in chitin can be reduced or broken, and the existence of alkali can enhance the extent of decrystallization. It suggested that alkali-freezing treatment may be chosen as a convenient precursor for efficient modifications of chitin (Hu et al., 2007; Liu et al., 2009, 2010). In this paper, the effect of alkaline freezing–thawing cyclic treatment on the structure of regenerated chitin was evaluated by XRD, FTIR and TG, and the structure changes before and after polymerization was also investigated.

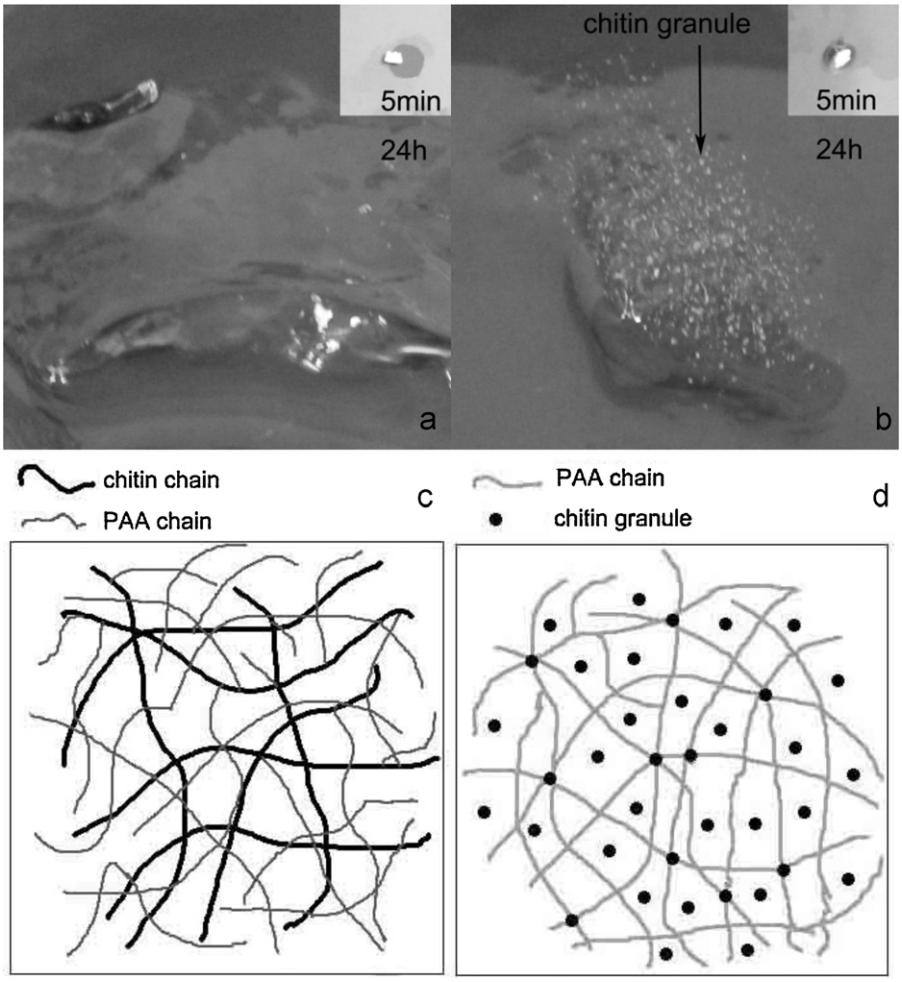


**Fig. 1.** Photographs and schematic structure of (a, c) SAP1 and (b, d) SAP2, respectively.

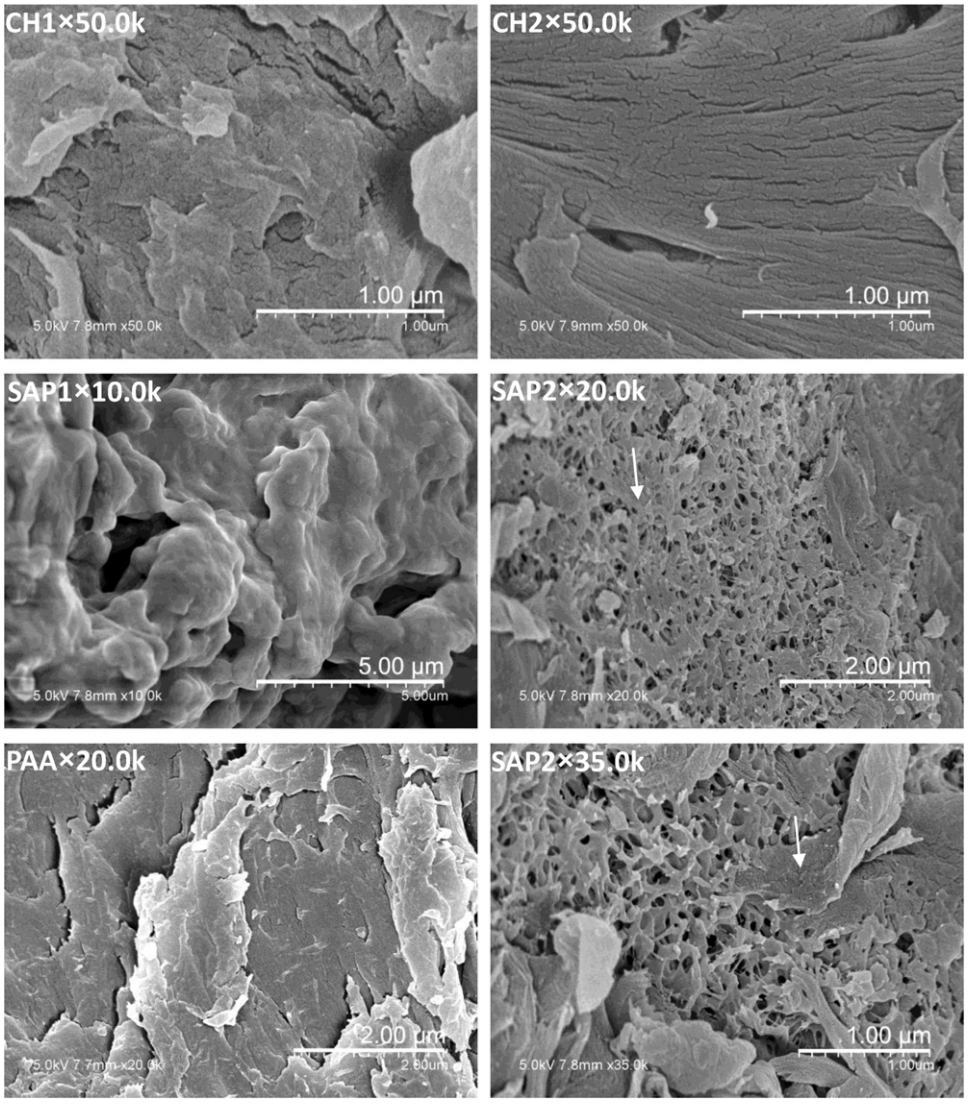


**Fig. 2.** SEM micrographs of regenerated chitin (CH1, CH2), superabsorbent polymers (SAP1, SAP2) and PAA, respectively.

*3.3.1. XRD patterns*

The XRD patterns of raw chitin (CH0), regenerated chitin (CH1 and CH2), superabsorbent polymers (SAP1 and SAP2) and PAA were given in Fig. 3. In CH0 five crystalline diffraction peaks at 9.53°, 19.46°, 20.79°, 23.39° and 26.52° were observed in the 2$\theta$ range of 4–30°, which were indexed as (0 2 0), (1 1 0), (1 2 0), (1 0 1), and (1 3 0), respectively, indicating that raw chitin is α-chitin, in accord with reported values (Hu et al., 2007; Liu et al., 2010). It denoted that the diffraction peaks decreased dramatically after FTC treatment, the peaks at 20.79° and 23.39° almost disappear, suggesting that the crystal structure was radically distorted during the FTC treatment. For the grafted polymer prepared under homogeneous conditions (SAP1), the diffraction pattern is highly similar to PAA. Compared with the pattern of CH1, the sharp crystalline reflections of chitin were concealed, and only observed a broad diffuse scattering peak. It indicated that the graft copolymerization reaction under homogeneous conditions was thoroughly. Moreover, the hydrogen bonding ability of chitin decreased after the grafting of PAA onto chitin backbone (Wang et al., 2008).

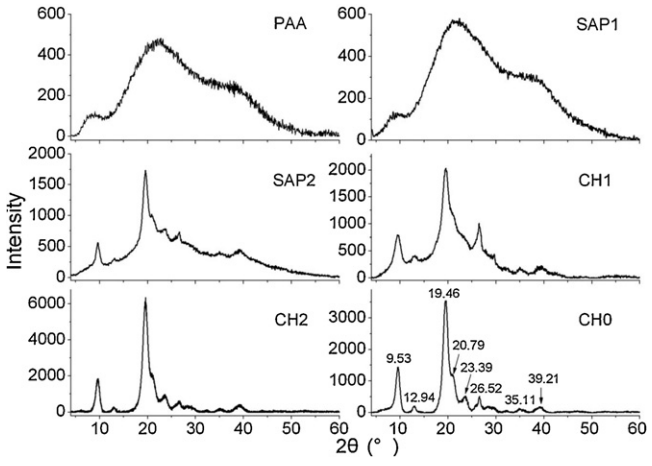


**Fig. 3.** XRD patterns of PAA, superabsorbent polymers (SAP1, SAP2), regenerated chitin (CH1, CH2) and original chitin (CH0), respectively.

However, the chitin solution was actually heterogeneous solution that obtained in accordance with the method reported throughout the literature (Hu et al., 2007). The intensity of the diffraction peaks in CH2 considerably enhanced instead of diminished. This is noticeably different from the previous reported data, and the factors were still fuzzy and required further study. For the grafted polymer (SAP2), the intensity of the diffraction peak was significantly attenuated compared to CH2. Whereas the diffraction pattern was also greatly similar to CH2, and it was significantly

different from PAA. This result again proved that the SAP2 was highly different from SAP1, and the PAA chains only were grafted onto the surface of the chitin particles.

### 3.3.2. FTIR spectra

In this study, FTIR analysis was applied to investigate the chemical structure of chitin, SAPs and the structure of SAPs changed with a different ratio of CH to AA. The major absorption peaks and their ascription of chitin was largely discussed in the previous literature (Cho et al., 2000; Hu et al., 2007; Liu et al., 2009, 2010). It could be seen clearly in Fig. 4 A that the absorption band at 3439 $cm^{-1}$ in chitin was referenced as OH stretching and the absorption of intra-hydrogen bonds (Hu et al., 2007), became broader, weaker and shifted to a lower wavenumbers after alkali-freezing treatment. The absorption peaks at 3267 and 3107 $cm^{-1}$ assigned to the N—H stretching vibration absorption were correspondingly weakened, and CH1 weakened more serious than CH2, in CH1 they virtually disappeared. The decrease of peak at 3267 $cm^{-1}$ indicated the reduction of intermolecular $C(2_1)NH\cdots O{=}C(7_3)$ hydrogen bonds, and the decrease of peak at 3107 $cm^{-1}$ indicated the reduction of intermolecular $C(6_1)OH\cdots HOC(6_2)$ hydrogen bonds (Cho et al., 2000). It also implied that antiparallel arrangement of the chains in raw chitin transforms to parallel arrangement in CH1 and CH2. It may be possible to conclude that the FTC treatment was more suited to significant undermine the hydrogen bond interaction of chitin molecules, which was helpful to improve the efficiency of graft polymerization. For CH2, the destruction of hydrogen bonds was inconspicuous compared with CH1. It could create a limited homogeneous environment on the surface or shallow surface of chitin particles. And it could be conducive to promoting the dissolution of chitin in alkaline solution, which would help the PAA chain to be grafted onto the surface of the chitin particle.

The FT-IR spectra of SAP1 and PAA in Fig. 4A were virtually identical. Compared with CH1, after graft polymerization, the absorption peak at around 3439 $cm^{-1}$ was attributed to the weakened and narrowed stretching vibration of —OH. As can be seen, the absorption bands at 3267 $cm^{-1}$, 3107 $cm^{-1}$ were ascribed to N—H stretching vibration, 1657 $cm^{-1}$ to C=O stretching vibration of amide I and 1314 $cm^{-1}$ to C—N stretching vibration and N—H in-plane bending vibration of amide III all disappeared. The absorption peaks at 1156 $cm^{-1}$ and 1073 $cm^{-1}$ showed the cancelation of the existence of the C—O—C bond. This information revealed that —OH, $—NH_2$, —NHCO and C—O—C of chitin took part in graft copolymerization reaction with AA. The diversity of the hydrophilic groups gave rise to a relatively substantial increase in water absorbent of the products. However, the intensity of the absorption band at 1560 $cm^{-1}$ was attributed to the unobvious weakened bending vibration of the N—H bond of amide II, suggesting that the amide groups might not be the primary reactive groups. Furthermore, after graft polymerization, a series of new absorption bands appeared in SAP1 at 2560 $cm^{-1}$, 1718 $cm^{-1}$, 1249 $cm^{-1}$, 808 $cm^{-1}$ and 621 $cm^{-1}$. Which were ascribed to N—H stretching, the symmetric stretching vibration of C=O in the —COOH groups, the C—O stretching vibration of the $—CH_2COOH$ groups, the planar rocking vibration of C—H of the long carbon chain and the C=O out of plane bending vibration, respectively. It indicated that the PAA chain grafted onto chitin backbone successfully, and the urea might also participate in the graft copolymerization reaction (Chen and Tan, 2006; Zhang et al., 2007). Meanwhile, the peak at 2892 $cm^{-1}$ corresponded to the C—H stretching vibration was overlapped by the peak at 2935 $cm^{-1}$, which was assigned to the $CH_3$ symmetrical stretching vibration and $CH_2$ asymmetrical stretching vibration, and the intensity of which increased, as a result of the introduction of the long carbon chain (Chen et al., 2009).

The FTIR spectra of SAP1 with a different ratio of chitin to AA is shown in Fig. 4B. The intensity of absorption bands at 1378 $cm^{-1}$ (the C—H bending vibration and $—CH_3$ symmetrical deformation vibration), 1150 $cm^{-1}$, 1070 $cm^{-1}$, 1031 $cm^{-1}$ and 897 $cm^{-1}$ (stretching vibration of the saccharide ring units) decreased gradually. Nevertheless, the intensity of absorption bands at 2560 $cm^{-1}$, 1718 $cm^{-1}$ and 1249 $cm^{-1}$ increased simultaneously. And the spectrum of SAP1 became more similar to PAA. All these results indicated that AA successfully grafted onto chitin backbone.

However, the spectrum of SAP2 in Fig. 4A was slightly different from SAP1. Besides of the characteristic absorption peaks of PAA, some intrinsic absorption peaks of chitin still can be obviously observed, such as 3267 $cm^{-1}$, 3107 $cm^{-1}$, 1657 $cm^{-1}$, 1156 $cm^{-1}$, 1070 $cm^{-1}$, 897 $cm^{-1}$, confirming again the graft copolymerization reaction under heterogeneous conditions was not completed, which was in conformity with the SEM and XRD results.

In order to assess the influence of alkali-freezing treatment on the condensed structure of chitin and the graft polymerization under different ratio of CH to AA more clearly, the spectra of regenerated chitin and SAP1 in the regions of 2200–4000 $cm^{-1}$ were first normalized based on unchanging total intensity. After normalization, the curves that mathematically best fitted to the original spectrum were obtained by the Gaussian function, with the software of the PeakFit Suite (Version 4.12, SeaSolve Software Inc., USA), and separated into each component peak of a symmetric nature associated with $r^2 > 0.9900$, as shown in Fig. 4C. Indeed, it was illustrated clearly that the absorption band at 3448 $cm^{-1}$ in chitin could be divided into two single peaks, as 3430 $cm^{-1}$ and 3489 $cm^{-1}$, which were assigned to the inherent OH and free OH stretching, respectively (Liu et al., 2010). For CH1, after FTC treatment the band at 3489 $cm^{-1}$ became broader and weaker with a shift to higher wavenumbers, but the band at 3430 $cm^{-1}$ almost did not change. In CH2, the band at 3489 $cm^{-1}$ shifted to higher wavenumbers, while the band at 3430 $cm^{-1}$ shifted to lower with an insignificant shift. Furthermore, the bands at 3102 $cm^{-1}$ both in CH1 and CH2 became weaker and broader after alkali-freezing, and the change of CH1 was more apparent. However, in the initial spectrum of CH1 (in Fig. 4A), those absorption bands were almost concealed. As can be seen, after graft polymerization, the intensity of the peak at 3266 $cm^{-1}$ in CH1 weakened gradually with the increase of the amount of AA, and the band at 3102 $cm^{-1}$ kept constant. The two bands in SAP2 were distinct from SAP1, and the band at 3093 $cm^{-1}$ became broader than CH2.

### 3.3.3. Thermal stability

The thermal properties of original chitin (CH0), regenerated chitin (CH1 and CH2), superabsorbent polymers (SAP1 and SAP2) and PAA were examined by thermogravimetric analysis (TGA). The TG, DTG and DTA curves were given and compared in Fig. 5. There was a definite weight loss (69%) in CH0 with the temperature increasing from 222.9 to 413.9 °C. The decomposition rate reached a maximum at 308.9 °C, which was attributed to the dehydration of the saccharide rings and breaking of the C—O—C glycosidic bonds in the main chain of the polysaccharide. With a further increase of the temperature to 600 °C, the weight of sample decreased to 5%, which was ascribed to the charring and thorough decomposition of pyranose residues. The thermal properties of CH2 were greatly similar to CH0, a sharp weight loss with increasing temperature from 173 to 415 °C and 71% of the sample was lost with a maximum decomposition rate at 315.9 °C. It can be concluded that the compact crystal structure was destructed insignificant after treatment according to the literature method (Hu et al., 2007), which was in conformity with the XRD results. The thermal behavior of CH1 is highly different from CH0 and CH2, and the peak at 300.6 °C of DTG curve with about 64% weight loss is broader than CH0 and CH2. Furthermore, the total weight loss of CH1 (approximately 99.6% of the initial sample) in the whole temperature range is larger than CH0 and CH2. It indicated that there was the more amorphous structure

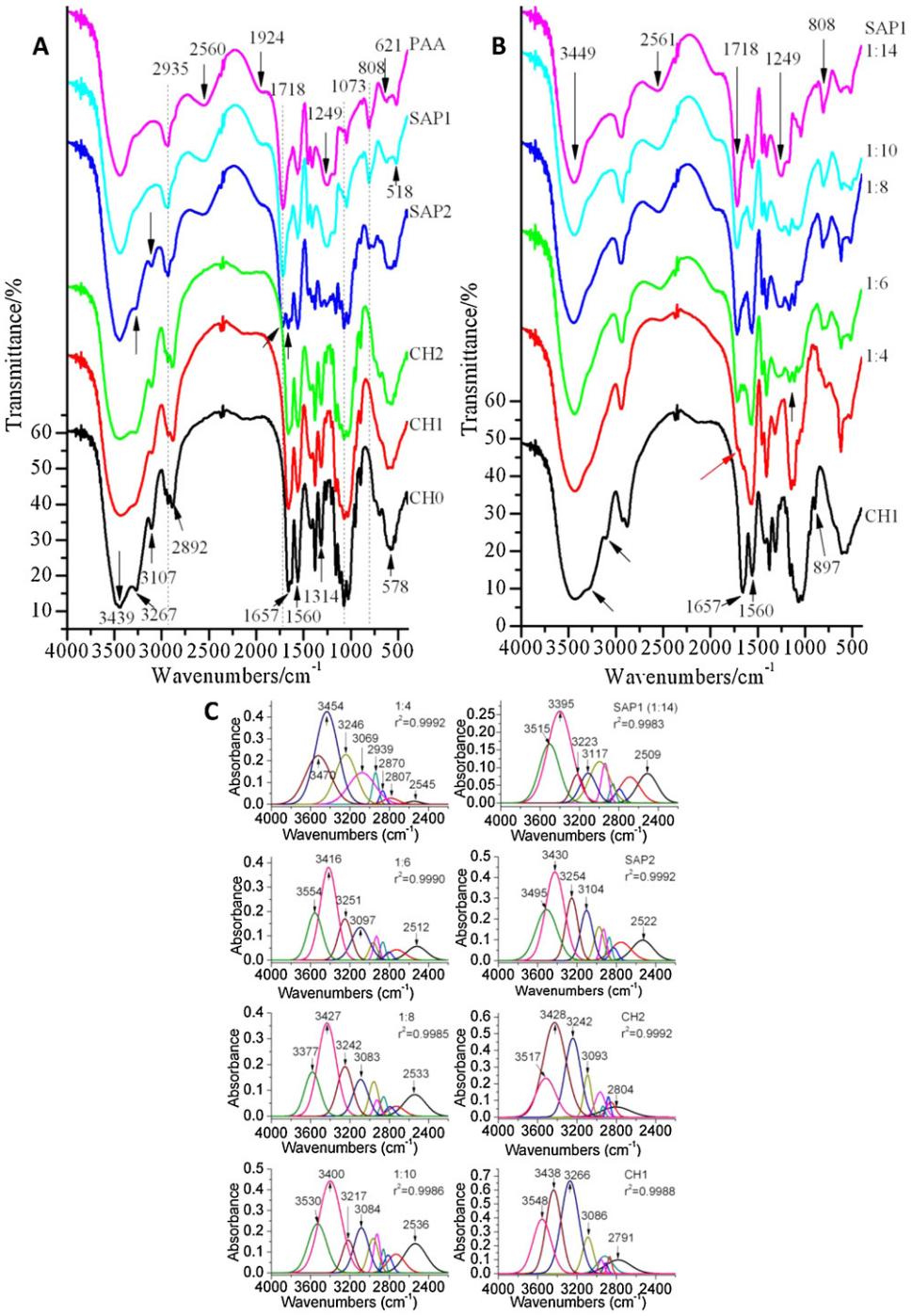


**Fig. 4.** FT-IR spectra (A, chitin, SAPs sample and PAA; B, CH1 and SAP1 with different ratio of CH and AA) and curves fitting (C) of chitin and SAPs, respectively.

in CH1, and its degradation rate was faster than the CH0 and CH2. It can also be revealed that the FTC treatment can destruct the crystal structure of chitin more sharply.

The thermal decomposition process of PAA was divided into four steps with a total mass loss of 82.79%. 10.59% mass loss during the first-stage decomposition was due to the evaporation of absorbed water molecules, 18.54% during the second to the decomposition of the carboxyl groups of PAA, 41.00% during the third to the rupture of the PAA chain, and 12.66% during the final step to the oxidative decomposition of the propylene residues (Chen and Tan, 2006). The thermic properties of SAP1 were similar to PAA with a total mass loss of 87.70%, which was greater than that of the PAA, and a higher maximum decomposition rate temperature than PAA, suggesting that the introduction of the chitin chain can improve the thermal stability of the graft copolymer. No obvious signal for the decomposition of chitin was observed in SAP1, it can also be divided into four steps. When the temperature increased from 24 to 246 °C, about 13.79% sample was lost due to the evaporation of absorbed water. Immediately, after that, decarboxylation of PAA and deamination of chitin started with a 22.71% mass loss reaching a maximum decomposition rate at 268 °C. The third stage was attributed to the rupture of the chitin-g-PAA chain with a mass loss of 35.41%, and the final step was due to the oxidative decomposition of the propylene and pyranose residues with a mass loss of 15.79%. However, the thermal properties of SAP2 were different from SAP1 and PAA, and an apparent signal for the decomposition of chitin was observed. The

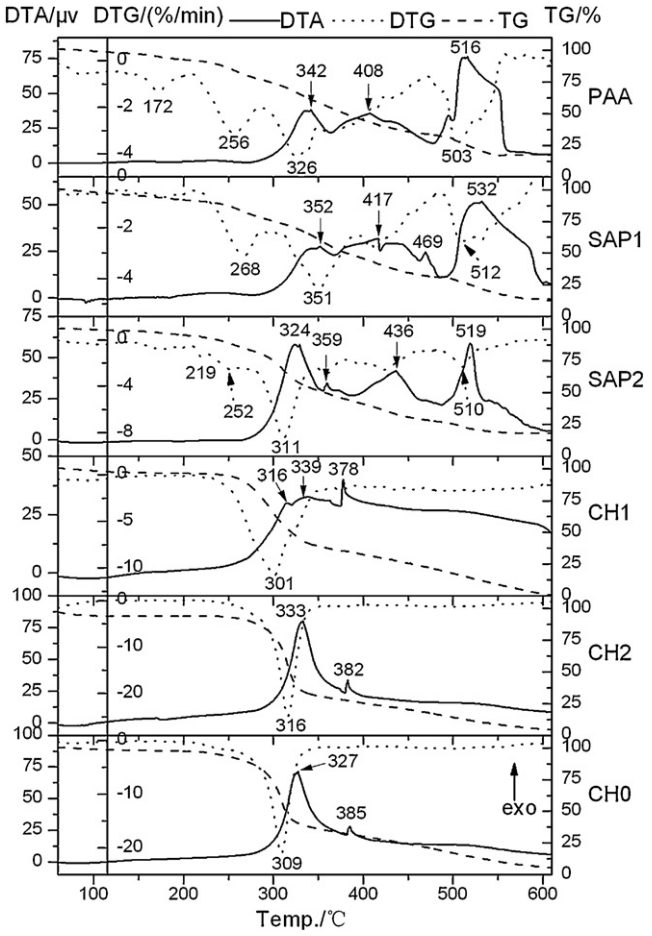


**Fig. 5.** TG, DTG and DTA curves of chitin, SAPs and PAA, respectively.

thermal decomposition process of SAP2 was divided into five steps with a total mass loss of 82.79%. 6.15% mass loss during the first step was due to the evaporation of absorbed water, which was lower than that of PAA and SAP1, 17.35% during the second to the decomposition of carboxyl groups, 20.70% during the third to the decomposition of chitin and PAA chain with the maximum decomposition rate being at 311 °C. 30.87% during the fourth step due to the decomposition of PAA chain, 7.72% during the final step was also owing to the oxidative decomposition of the propylene and pyranose residues.

## 4. Conclusions

FTC treatment can substantially undermine the compacted crystal structure and hydrogen bonding of chitin. The effect of which is better than the alkali-freezing treatment used alone. It helps the chitin to dissolve in NaOH/urea solution, and a really homogeneous alkalic chitin solution can be obtained. The static solution polymerization method was applied to prepare a chitin-g-PAA superabsorbent polymer using the alkaline chitin solution directly in a thermo-constant water bath without nitrogen protection. APS was used as an initiator and MBA was used as a crosslinker. Structural analysis showed that AA successfully grafted onto the chitin molecule chain, and it revealed that the SAPs were possessed of more amorphous structure but with good thermal stability. Direct preparation of superabsorbent polymers using chitin as a raw material helped to retain the unique physical and chemical properties and biological activities of chitin. In chitin molecular, the more hydrophilic groups (such as $-NH_2$, $-NHCOCH_3$, —OH, etc.) involved in the graft copolymerization reaction, it is possible to significantly improve the water absorption of the product. The absorption capacity of SAP prepared under optimum conditions reached to 2833 g/g in distilled water, it can form a transparent and uniform gel without any residual chitin particles. Furthermore, NaOH and urea not only play the role of solvent, but also involved as the reaction reagents. Acrylic acid without prior neutralization can simplify the procedures and reduce the water consumption. Therefore, the final product exists as a hydrogel without excess reagent emissions, which is conducive to reducing the environmental pollution. The polymerization reaction can be carried out in a small beaker without nitrogen to remove oxygen, and it can also simplify the synthesis procedures considerably. It indicated that this preparation procedure is a convenient method, which is a potential method for industrial application's pathway.

## Acknowledgments

The authors are grateful to the support of the Chinese National Foundation of Natural Sciences (Nos. 21271035 and 21071024), the Natural Science Foundation of Anhui Provincial Education Department (No. KJ2011B110) and the Key Disciplines of Materials Science in Chizhou University (Nos. 2011XK04 and 2012CL001).

## References

Austin, P. R., Brine, C. J., Castle, J. E., & Zikakis, J. P. (1981). Chitin: New facets of research. *Science*, *212*(4496), 749–753.
Chang, C. Y., Chen, S., & Zhang, L. N. (2011). Novel hydrogels prepared via direct dissolution of chitin at low temperature: Structure and biocompatibility. *Journal of Materials Chemistry*, *21*(11), 3865–3871.
Chang, C. Y., Duan, B., Cai, J., & Zhang, L. N. (2010). Superabsorbent hydrogels based on cellulose for smart swelling and controllable delivery. *European Polymer Journal*, *46*(1), 92–100.
Chen, Y., Liu, Y. F., Tan, H. M., & Jiang, J. X. (2009). Synthesis and characterization of a novel superabsorbent polymer of N, O-carboxymethyl chitosan graft copolymerized with vinyl monomers. *Carbohydrate Polymers*, *75*(2), 287–292.
Chen, Y., & Tan, H. M. (2006). Crosslinked carboxymethylchitosan-g-poly(acrylic acid) copolymer as a novel superabsorbent polymer. *Carbohydrate Research*, *341*(7), 887–896.
Cho, Y. W., Jang, J. H., Park, C. R., & Ko, S. W. (2000). Preparation and solubility in acid and water of partially deacetylated chitins. *Biomacromolecules*, *1*(4), 609–614.
Ding, B. B., Cai, J., Huang, J. C., Zhang, L. N., Chen, Y., Shi, X. W., et al. (2012). Facile preparation of robust and biocompatible chitin aerogels. *Journal of Materials Chemistry*, *22*(12), 5801–5809.
Elkholy, S., Khalil, K. D., Elsabee, M. Z., & Eweis, M. (2007). Grafting of vinyl acetate onto chitosan and biocidal activity of the graft copolymers. *Journal of Applied Polymer Science*, *103*(3), 1651–1663.
Furlan, L., Fávere, V. T., & Laranjeira, M. C. M. (1996). Adsorption of calcium ions by graft copolymer of acrylic acid on biopolymer chitin. *Polymer*, *37*(5), 843–846.
Hsu, S. C., Don, T. M., & Chiu, W. Y. (2002). Free radical degradation of chitosan with potassium persulfate. *Polymer Degradation and Stability*, *75*(1), 73–83.
Hsu, S. T., Lin, W. C., Hsiao, W. F., Lee, C. C., Pan, T. C., Wang, T. T., et al. (2013). Preparation of methacrylic acid-grafted chitin using cerium (IV) ion and its application in adsorbing paraquat. *Journal of Applied Polymer Science*, *127*(1), 760–764.
Hu, X. W., Du, Y. M., Tang, Y. F., Wang, Q., Feng, T., Yang, J. H., et al. (2007). Solubility and property of chitin in NaOH/urea aqueous solution. *Carbohydrate Polymers*, *70*(4), 451–458.
Ifuku, S., Iwasaki, M., Morimoto, M., & Saimoto, H. (2012). Graft polymerization of acrylic acid onto chitin nanofiber to improve dispersibility in basic water. *Carbohydrate Polymers*, *90*(1), 623–627.
Kim, J. Y., Ha, C. S., & Jo, N. J. (2002). Synthesis and properties of biodegradable chitin-graft-poly(L-lactide) copolymers. *Polymer International*, *51*(10), 1123–1128.
Kurita, K., Kawata, M., Koyama, Y., & Nishimura, S. I. (1991). Graft copolymerization of vinyl monomers onto chitin with cerium (IV) ion. *Journal of Applied Polymer Science*, *42*(11), 2885–2891.
Lin, S. B., Lin, Y. C., & Chen, H. H. (2009). Low molecular weight chitosan prepared with the aid of cellulase, lysozyme and chitinase: Characterisation and antibacterial activity. *Food Chemistry*, *116*(1), 47–53.
Liu, J. H., Wang, H., & Wang, A. Q. (2007). Synthesis and characterization of chitosan-g-poly(acrylic acid)/sodium humate superabsorbent. *Carbohydrate Polymers*, *70*(2), 166–173.
Liu, T. G., Li, B., Huang, W., Lv, B., Chen, J., Zhang, J. X., et al. (2009). Effects and kinetics of a novel temperature cycling treatment on the N-deacetylation of chitin in alkaline solution. *Carbohydrate Polymers*, *77*(1), 110–117.
Liu, T. G., Li, B., Zheng, X. D., Liang, S., Song, X., Zhu, B., et al. (2010). Effects of freezing on the condensed state structure of chitin in alkaline solution. *Carbohydrate Polymers*, *82*(3), 753–760.

Ma, Z. H., Li, Q., Yue, Q. Y., Gao, B. Y., Xu, X., & Zhong, Q. Q. (2011). Synthesis and characterization of a novel super-absorbent based on wheatstraw. *Bioresource Technology*, *102*(3), 2853–2858.

Muzzarelli, R. A. A. (2011). Biomedical exploitation of chitin and chitosan via mechano-chemical disassembly, electrospinning, dissolution in imidazolium ionic liquids, and supercritical drying. *Marine Drugs*, *9*(9), 1510–1533.

Muzzarelli, R. A. A. (2012). Nanochitins and nanochitosans, paving the way to eco-friendly and energy-saving exploitation of marine resources. In K. Matyjaszewski, & M. Möller (Eds.), *Polymer science: A comprehensive reference* (pp. 153–164). Amsterdam: Elsevier B.V.

Muzzarelli, R. A. A., Boudrant, J., Meyer, D., Manno, N., DeMarchis, M., & Paoletti, M. G. (2012). Current views on fungal chitin/chitosan, human chitinases, food preservation, glucans, pectins and inulin: A tribute to Henri Braconnot, precursor of the carbohydrate polymers science, on the chitin bicentennial. *Carbohydrate Polymers*, *87*(2), 995–1012.

Nakason, C., Wohmang, T., Kaesaman, A., & Kiatkamjornwong, S. (2010). Preparation of cassava starch-graft-polyacrylamide superabsorbents and associated composites by reactive blending. *Carbohydrate Polymers*, *81*(2), 348–357.

Pillai, C. K. S., Paul, W., & Sharma, C. P. (2009). Chitin and chitosan polymers: Chemistry, solubility and fiber formation. *Progress in Polymer Science*, *34*(7), 641–678.

Sadeghi, M., & Ghasemi, N. (2012). Synthesis and study on effect of various chemical conditions on the swelling property of collagen-*g*-poly(AA-*co*-IA) superabsorbent hydrogel. *Indian Journal of Science and Technology*, *5*(1), 1879–1884.

Sadeghi, M., & Hosseinzadeh, H. (2010). Synthesis and super-swelling behavior of a novel low salt-sensitive protein-based superabsorbent hydrogel: Collagen-*g*-poly (AMPS). *Turkish Journal of Chemistry*, *34*(5), 739–752.

Tanodekaew, S., Prasitsilp, M., Swasdison, S., Thavornyutikarn, B., Pothsree, T., & Pateepasen, R. (2004). Preparation of acrylic grafted chitin for wound dressing application. *Biomaterials*, *25*(7–8), 1453–1460.

Wang, J. P., Chen, Y. Z., Zhang, S. J., & Yu, H. Q. (2008). A chitosan-based flocculant prepared with gamma-irradiation-induced grafting. *Bioresource Technology*, *99*(9), 3397–3402.

Yang, L. L., Ma, X. Y., & Guo, N. N. (2011). Synthesis and properties of sodium alginate/$Na^+$ rectorite grafted acrylic acid composite superabsorbent via $^{60}Co\gamma$ irradiation. *Carbohydrate Polymers*, *85*(2), 413–418.

Yazdani-pedram, M., Lagos, A., Campos, N., & Retuert, J. (1992). Comparison of redox initiators reactivities in the grafting of methyl methacrylate onto chitin. *International Journal of Polymeric Materials*, *18*(1–2), 25–37.

Yoshimura, T., Uchikoshi, I., Yoshiura, Y., & Fujioka, R. (2005). Synthesis and characterization of novel biodegradable superabsorbent hydrogels based on chitin and succinic anhydride. *Carbohydrate Polymers*, *61*(3), 322–326.

Zhang, B. N., Cui, Y. D., Yin, G. Q., & Zhou, H. B. (2011). Preparation of cottonseed protein-based superabsorbent hydrogel composite. *Advanced Materials Research*, *328–330*, 1589–1593.

Zhang, B. N., Cui, Y. D., Yin, G. Q., Li, X. M., Liao, L. M., & Cai, X. B. (2011). Synthesis and swelling properties of protein–poly(acrylic acid-co-acrylamide) superabsorbent composite. *Polymer Composites*, *32*(5), 683–691.

Zhang, J. P., Wang, H., & Wang, A. Q. (2007). Synthesis and characterization of chitosan-*g*-poly(acrylic acid)/attapulgite superabsorbent composites. *Carbohydrate Polymers*, *68*(2), 367–374.

Zou, W., Yu, L., Liu, X. X., Chen, L., Zhang, X. Q., Qiao, D. L., et al. (2012). Effects of amylose/amylopectin ratio on starch-based superabsorbent polymers. *Carbohydrate Polymers*, *87*(2), 1583–1588.